Bioelectrochemistry 144 (2022) 108028

Contents lists available at ScienceDirect

Bioelectrochemistry

journal homepage: www.elsevier.com/locate/bioelechem

Cells electric charge analyses define specific properties for cancer cells activity

J.A. Moleón Baca [a,*], A. Ontiveros Ortega [a], A. Aránega Jiménez [b], S. Granados Principal [c]

[a] Department of Physics, University of Jaén, Spain
[b] Department of Experimental Biology, University of Jaén, Spain
[c] GENYO, Centre for Genomics and Oncological Research, Pfizer, University of Granada, Spain.

ARTICLE INFO

Article history:
Received 28 July 2021
Received in revised form 25 November 2021
Accepted 28 November 2021
Available online 1 December 2021

Keywords:
Interaction energy between tumour cells
Zeta potential
Surface free energy

ABSTRACT

The surface electrical charge of cells is conditioned by the ionic medium in which they are immersed. This charge is specific for each cell type and is especially important in tumour cells because it determines their state of aggregation and their adhesion in the different organs. This study analyses the variations in surface charge of cells when pH, electrolytes, and their concentration are modified. The modification of these factors leads to changes in the surface charge of tumour cells; therefore, their states of aggregation and behaviour can be modified. This may even have a use in the prognosis and treatment of various tumours. Some studies conclude that the activity associated with the glycolysis process is accompanied by a change in the surface charge of cells. Notably, there is a high rate of glycolysis in tumours. Our results show that surface charge of cells strongly depends on nature of ionic medium in which they are found, with the valence of the majority ion being the most important factor. When ionic strength was high, the charge decreased dramatically. On the other hand, charge becomes zero or positive in an acidic pH, while in a basic pH, the negative charge increases.

1. Introduction

Currently, various interesting lines of research in cancer diseases focus on markers that can distinguish diseased cells from normal ones, and many research groups around the world work on this goal in different ways [1–6]. We have paid particular attention to the electrical properties of the cell surface. Cell surface charge is one of the important parameters affecting its relationship with other cells as well as the adsorption and absorption processes in the cell membrane [7,8,9]. This parameter depends on several factors, including the physicochemical properties of the environment in which they are found [11]. Although cells are situated in a very complex medium and are difficult to control within the human body, knowing the conditions under which the surface charge of cells can be changed may lead to the control of tumour development and specific treatments.

Tumour processes appear to be accompanied by an increase in the negative charge of the cell surface due to the glycolysis process [12]. In addition, studies of the electrical surface properties of biological cells are also providing knowledge on resulting cell behaviour [10]. Hence, depending on the state of the cell and its biological functions, the surface properties may change.

This study aimed to determine the surface properties (electrical and thermodynamic) of tumour cells under strict control of the ionic strength and pH of the medium. In parallel, the same analyses have been carried out with normal cells to verify the analysis. This study investigates the essential step prior to determining what mechanisms allow us to modify or inhibit the surface charge of the tumour cells, thus enabling intervention in the tumour process.

Clearly, the cells' surface properties may influence tumour growth or cancer cell aggregation; therefore, this study aimed to determine the surface properties of both normal and tumour cells and determine how they change.

2. Materials and methods

2.1. Cell lines

2.1.1. Tumour cell line

A positive oestrogen receptor (MCF-7) breast cancer cell line was obtained from the American Type Culture Collection (ATCC). Cells were grown in DMEM (Gibco) supplemented with 10% of foetal bovine serum (ThermoScientific) and 1% of antibiotic - antifungal (Gibco) at 37 °C with 5% CO_2. The cell line was not tested or

* Corresponding author.
E-mail addresses: jamoleon@ujaen.es (J.A. Moleón Baca), aontiver@ujaen.es (A. Ontiveros Ortega).

https://doi.org/10.1016/j.bioelechem.2021.108028
1567-5394/

authenticated beyond the documentation provided by the ATCC, which includes antigen expression, DNA profile, short tandem repeat profile, and cytogenic analysis. Cell proliferation was evaluated with the WST-1 method assay.

The Phosphate Buffered Saline Solution (PBS) was used as a neutral vehicle to keep the cells alive until they were diluted to the required ionic concentrations for measurements.

2.1.2. Sol8 and C2C12 cell lines

Sol8 is a myogenic cell line isolated by Daubas et al. from primary cultures of soleus muscle taken from the leg of a normal C3H mouse [13]. C2C12 is a subclone from a myoblast line established from normal adult C3H mouse leg muscle [14,15]. Sol8 and C2C12 cell lines were provided by the ATCC. Both cell lines were cultured in growth medium (GM) consisting of DMEM supplemented with 10% foetal bovine serum, 2 mM L-glutamine, and 50 U/ml penicillin–streptomycin, as previously described [16,17].

2.2. Zeta potential ζ

The electrokinetic properties of the studied systems were analysed with a Malver-ZetaSizer 3000 HS. For each treatment, the tumour cells were conditioned with the solutions, at the required ionic concentrations and pH, for 10 min before the measurements. For electrophoretic mobility, the cells were redispersed in the ionic solution required for the experiment at an approximate concentration of 5000 cells/cm^3.

The state and concentration of the samples to be measured were verified by optical microscopy before measurements were taken (Fig. 1). In Fig. 1, the clear morphology of the cells can be observed; the tumour cells have a highly spherical geometry even when deposited on the microscope plate (Fig. 1.c). Fibroblasts showed a certain oval shape on the plate (Fig. 1.a and 1.b); however, they regained their spherical shape in solution.

Therefore, we applied the theoretical models provided for spherical symmetry in the double layer in both cases.

2.3. Surface free energy

To estimate the surface free energy of the samples, the advancing contact angles of three probe liquids (diiodomethane, water, and formamide) were measured. A Ramé-Hart Instrument Co. (New Jersey USA) NRL CA goniometer was used for these measurements. Drops were placed on the surface with a Gilmont (USA) micrometre syringe and images were captured immediately after with a video camera adapted to the goniometer. The contact angles of water, formamide, and diiodomethane were measured on a thin layer of cells deposited on a glass slide. The thin layer of cells having a smooth, specular surface (at the optical microscope level) was selected. The contact angle was recorded immediately after depositing the drop.

More information on the interface theory related to this type of system, together with the description of the interaction forces between particles, can be found in the Supplementary Materials.

3. Results and discussion

3.1. Electrical characterisation of Cells: Potential zeta

Figs. 2, 3, 4, and 5 show values of ζ as a function of pH for different electrolytes (monovalent, divalent, and trivalent) and concentrations. We used sodium chloride as the monovalent electrolyte because it is a common cation in blood serum and a reference cation in electrokinetic studies of inorganic and organic materials. We used calcium as a divalent cation because, in addition to being part of the blood serum, its concentration can affect certain pathologies. Finally, as a trivalent cation, we made measurements with iron and aluminium, whose variations in concentration accompany tumour processes.

Fig. 2 shows the results obtained for zeta potential at 10^{-2} M of sodium concentration as a function of pH for two normal cell lines (C2C12 and Sol 8) and breast tumour cells.

The results of the first cell line (C2C12) showed that tumour cells present less zeta potential (5 mV) than normal ones. This observation contradicts the results obtained by some authors [12], who reported that the glycolysis process results in an excess negative charge on the tumour cell. Another normal cell line was used (Sol8 P11) to verify these results, and which reconfirmed our C2C12 results. Fig. 2 shows that tumour cells reach the most negative zeta potential value of −15 mV in a neutral pH (pH 7). In comparison, normal ones reach values between −20 to −25 mV in a neutral pH and reach up to −30 mV in basic pHs.

In general, zeta potential values are negative for monovalent and divalent electrolytes, and other authors have obtained similar results [10,12]. This behaviour, in general, results from the balance between the ionic species inside and outside the cell membrane, which results in an excess negative charge on the surface.

The surface charge and therefore, the zeta potential of the cells result from the selective cell membrane permeability to some cations and an excess of anions inside the cell. This dynamic equilibrium generates variations in the membrane potential that are responsible for the majority of cellular functions. In this study, we do not focus on the charge generation mechanisms but on the possible effects of its existence on coagulation and adhesion phenomena. The physical background of charge generation in cell membranes is explained in detail in some references [18,19,20,21].

The charge values obtained for the cell membranes were modified by a change in the medium's pH, electrolytes, and electrolyte concentration. Some authors have observed that the cell membrane charge increases during tumorigenesis and decreases during necrosis [10,22,23], and that these changes are on the order of a few mV. This indicates that the electrophoretic measurement technique for charge determinations is suitable to study the evolutions of the tumour processes. In our results, the differences observed depended on the ionic strength, with variations of up to 15 mV at 1 mM de ClNa or 20 mV at 0.1 mM with a basic pH.

Fig. 3 shows the zeta potential (ζ) of cells for a pH between 3 and 10 at different Na^+ ionic strengths (10^{-3} to 10^{-1} M). The normal cells of the C2C12 line are represented in Fig. 3.a and breast tumour cells in Fig. 3.b.

For increasing pH values, the ζ potential was generally observed to increase in absolute values for all ionic strengths studied, except for the highest 10^{-1} M, which was practically zero (<2 mV). In addition, the increase in ionic strength was accompanied by a decrease, in the absolute value, of the ζ potential. This can be explained due to increased compression of the electric double layer. This compression is especially noticeable with the highest ionic strength used, where the compression of the double layer is such that zeta potentials are practically null for all pH values studied. Therefore, it can be seen that for higher ionic strengths, the charge of the cell is independent of the pH values.

Fig. 3.a corresponds to the data for normal cells. A progressive increase in the charge with pH values can be seen, probably due to the progressive absorption of hydroxyl groups on the cell surface. Fig. 3.b shows the obtained values for cancer cells. The zeta potential values of these cells present a similar trend to normal cells. The notable difference is that the zeta potentials are lower in absolute values than those of normal cells for all ionic strengths and pH's, around 10–15 mV. Similar results were obtained by Gogichadze [24]. This suggests that the absorption capacity of hydrogen

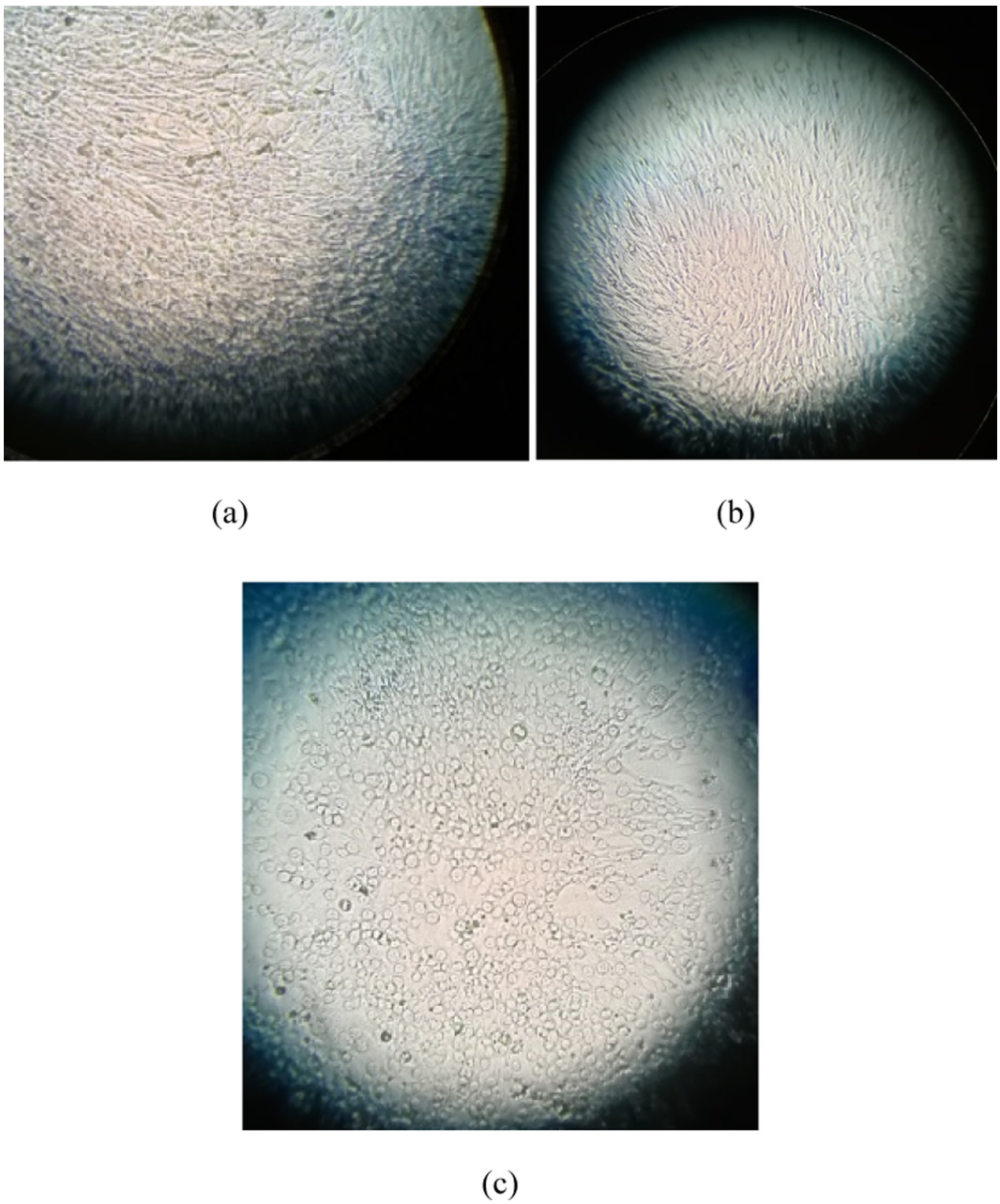

Fig. 1. Optical microscope photograph of the two normal cell lines and breast tumour cells: (a) cell line C2C12, (b) cell line Sol8P11, and (c) breast tumour cells.

ions (OH) is lower in tumour cells, resulting in lower zeta potential values.

Fig. 4 shows the effect of a divalent electrolyte (Ca^{++}) on the ζ potential values at different pH and ionic strengths for both cells line. In Fig. 4.a, first, we observed that for higher concentrations of electrolytes, the ζ potential decreases to zero, similar to the values presented for Na^{-} ions. Second, the superficial charge is practically constant with the different pH values in normal cells [25] (the variation of zeta potential is 0–2 mV). For higher ionic strengths (10^{-1} and 10^{-2} M), corresponding with the saline concentration of blood plasma, the ζ potential values were positive in all pH ranges. The highest measured values were around + 10 mV, corresponding to (10^{-2} M) of Ca^{++} ions. This is due to the progressive absorption of calcium onto the cell surface, decreasing the negative charge of the cell at low concentrations (10^{-3} M), with reversal of the charge sign for higher concentrations (10^{-2} M). In the case of low ionic strength (10^{-3}, 10^{-4} M), the ζ potential values are positives for acid pH and negatives for basic pH levels. This charge behaviour is an interesting result for interpreting the mechanism of interaction between similar cells or cells of a different nature. That is, the electrostatic interaction energy is repulsive between similar cells and either attractive or repulsive in adhesion processes between different bodies, depending on whether the ionic strength is 10^{-2} or 10^{-3} of $CaCl_2$, or depending on the pH for the concentration of 10^{-1}.

Fig. 4.b shows the obtained results for cancer cells. A progressive decrease of zeta potential values was observed with an increasing calcium concentration, probably due to the absorption of Ca^{++} ions. In all cases, the absorption process was less than for the normal cells but never reversing the charge.

The effect of trivalent electrolytes (Fe^{+++} and Al^{+++}) has been studied. In this case, the analysis of zeta potential was conducted

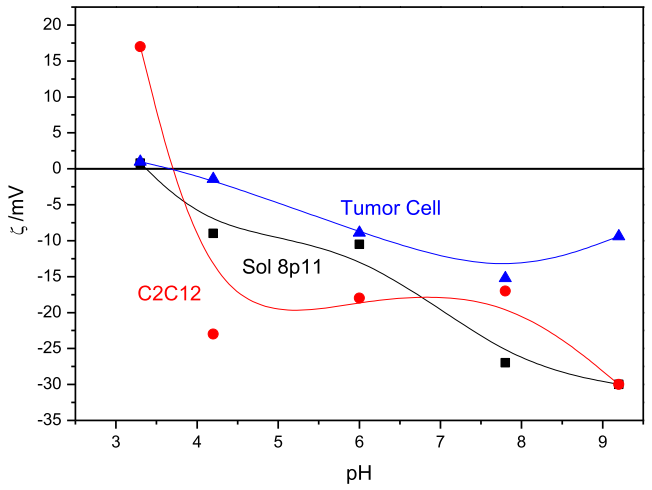

Fig. 2. Dependence of the zeta potential of the two normal cell lines and breast tumour cells at ionic strength 10^{-2} M of Na^{++}, as a function of the pH of the liquid phase.

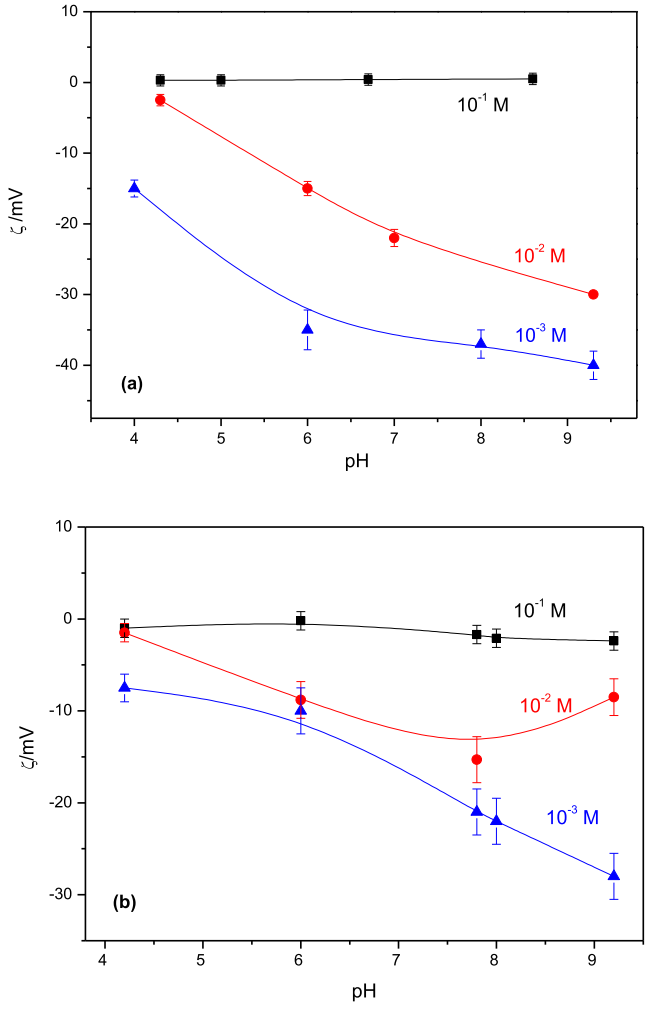

Fig. 3. Dependence of the zeta potential of cells for three ionic strength of Na^{+} (10^{-1}, 10^{-2}, and 10^{-3} M) as a function of pH of the liquid phase: (a) cell line C2C12 and (b) breast tumour cells.

in natural pH conditions because of the precipitation of complex ions, aluminium and iron, at a pH greater than 4. Fig. 5 shows the ζ potential values for different ionic strengths at pH≈4. In

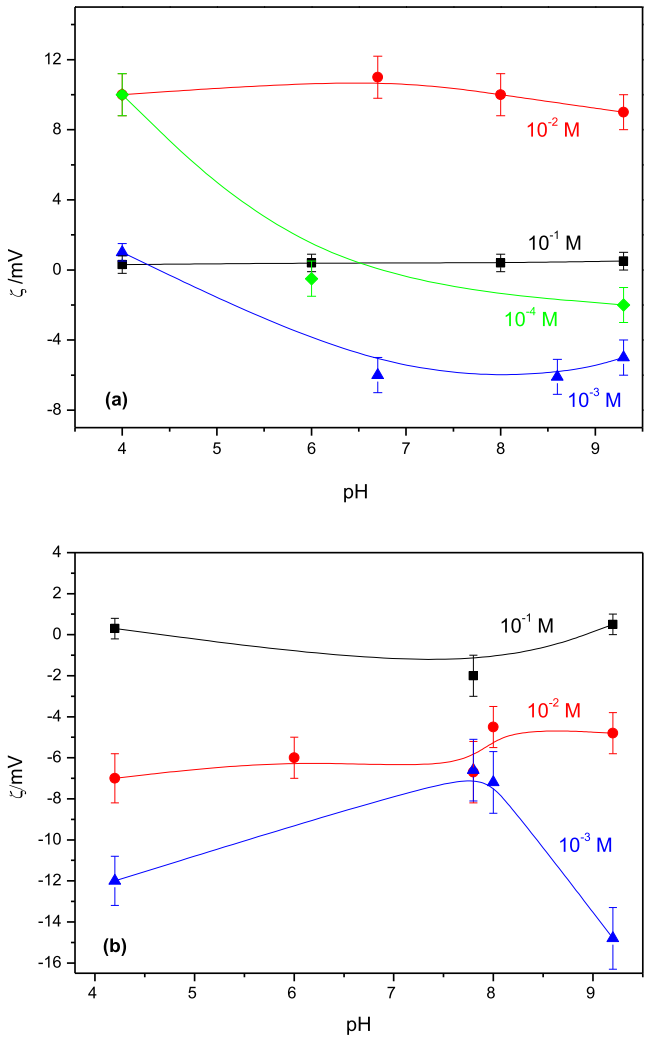

Fig. 4. Dependence of the zeta potential of cells for three ionic strength of Ca^{++} (10^{-1}, 10^{-2}, and 10^{-3} M) as a function of the pH of the liquid phase: (a) cell line C2C12 and (b) breast tumour cells.

general, the effect of a trivalent ion turns the ζ potential to a positive, related to precompensation of the charge near the charged surface [26].

Fig. 5.a shows the results for normal cells. Similar to the other electrolytes studied, at a higher concentration (10–1 M), the ζ potential was zero. In the case of physiologic saline concentration (10^{-2} M) we can see that the ζ potential values of Fe^{+++} go to + 33 mV, while for the Al^{+++} it is + 5 mV. At a lower concentration (10^{-3} M), the difference between the two values becomes small.

Fig. 5.b shows the zeta potential values for tumour cells versus normal cells. The zeta potential values were low for iron, indicating less absorption of this cation than aluminium in tumour cells. For both ions, the values were lower in normal cells than in tumour cells. The maximum value obtained for Al^{+++} was about 17 mV, while it was 25 mV for normal ones. This result is even more evident if we consider the Fe^{+++} cation: in tumour cells, the maximum is 27 mV, while in normal ones, it is 35 mV.

The results obtained for extreme concentrations of iron (10^{-3} and 10^{-1} M) stand out; greater zeta potential values were obtained for 10^{-1} M. This contradicts the general rule that a "higher ionic strength implies higher compression of the double layer and a lower zeta potential value." The lowest zeta potential values were obtained for very small ionic strength (5 mV) and higher values for highest ionic strength, of order of 10 mV.

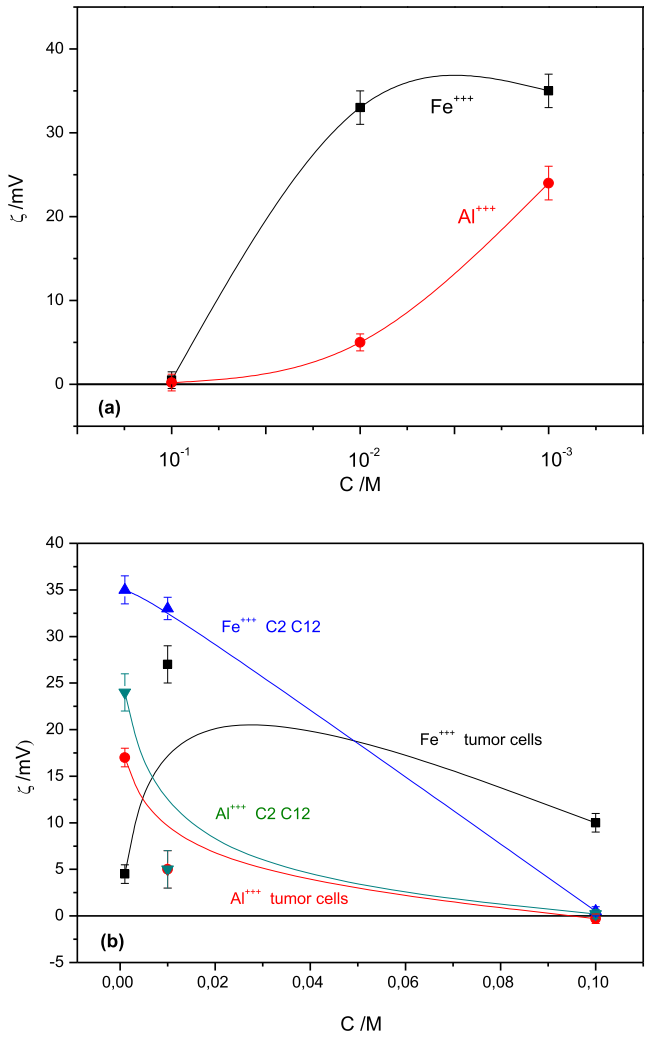

Fig. 5. Dependence of the zeta potential of cells for three ionic strengths of trivalent ions at pH≈4: (a) cell line C2C12 and (b) breast tumour cells versus normal cells.

Usually, for inorganic materials, this contradictory result is attributed to coagulation phenomena and, therefore, to the increase in the size of the suspended particles measured in the zeta-meter [27,30]. A plausible explanation would be to assume that cancer cells coagulate at high concentrations, and therefore, what is measured is not the zeta potential of individual particles but of aggregates; thus, the 12 mV would correspond to these possible aggregates.

Hence, knowing the surface charge of cancer cells may have important applications in studying and treating tumours. If it is assumed that the fixation in a certain organ of tumour cells from the bloodstream has an electrostatic component, then the sign of their surface charge would be of vital importance in the metastasis processes.

Furthermore, the results show that tumour cells do not have a fixed charge; on the contrary, this can change in magnitude and sign depending on the ionic medium and the pH in which it is found. We also consider that the analysis of the cell charge could be used as a diagnostic method or to detect or differentiate tumour cells [28].

3.2. Surface free energy

Above in this manuscript, cells have been characterised from the electrical point of view, and the interactions between cells and the aqueous medium considered as exclusively electrostatic. However, this study also considers other types of interactions between particles, specifically thermodynamic interactions, van der Walls, acid-base, and structural, which are especially interesting in biological systems [28]. In this sense, a first approximation of the novel methodology that can be used and some initial results that support its viability are presented here.

There are two methods to determine the van der Walls and acid-base interactions: the thin layer wicking, and the contact angle method. In our study, we used the contact angle method [29,31].

The adhesion between solid particles of colloidal size dispersed in aqueous media is determined by the balance of forces between various phases coexistent in a system: dispersive, polar, and electrical interactions. The first two are used for the approximation of particles and short distances. However, when there is appreciable electrical surface charge, the electrical interaction governs this phenomenon. Therefore, the study was conducted considering only the electrical component, leaving the result of the three components as an example, only for normal cells.

Table 1 shows surface tension and the surface tension component (mJ/m^2) of the liquid used in contact angle measurement. Table 2 lists the contact angles obtained for the different liquids used in our experiment (water, formamide, and diiodomethane), followed by the components of surface free energy obtained from them using Eq. (2) for the two normal cell lines studied.

The results from the contact angles show the habitual behaviours for the three liquids tested, and the differences between the angles for water and formamide for the two cell lines can be appreciated. Of note, Fibroblasts Sol 8P11 have a contact angle with water around 30° compared with 21° for Fibroblasts C2C12; suggesting that the first line has less wetting capacity. In terms of the surface free energy components, there was no appreciable difference between the dispersive Lifshitz-van der Waals (LW) components. Moreover, the value of the LW component is around 28 mJ/m^2 for both cell lines; this value is extremely low and very close to that of water (21.8 mJ/m^2). This indicates that both cell lines have a low capacity to structure the water molecules around their surface.

The analysis of the non-dispersive component, or acid-base component (γ^+ andγ^-), shows a monopolar character ($\gamma^+\approx 0$ and $\gamma^-\neq 0$) for both samples that is almost electron-donor in nature (γ^- between 40 and 60 mJ/m^2). There is also a difference of 14 mJ/m^2 between the two cells line. Given that monopolar material that is electron-donor in nature with $\gamma^- < 28$ mJ/m^2 [33] has a hydrophobic nature, and that the hydrophobicity or hydrophilic nature of a material is based on wetting behaviour, then this behaviour can be understood in terms of how the ionisable groups dissociate. These ionisable groups can be electron-donor or electron-acceptor in nature, depending on whether the cell gains a negative charge or on its wetting behaviour. The hydrophilicity of a cell can be understood in terms of how many ionisable groups exist on its surface. In this sense, the result shows that the cells' surface is hydrophilic nature ($\gamma^+\approx 0$ and $\gamma^- < 28$ mJ/m^2). In our results, Fibroblasts C2C12 presented a higher hydrophilic character than Fibroblasts Sol 8P11.

Table 2 also shows the total surface free energy for both cell lines. The two values are observed to be similar, indicating that the two fibroblasts lines have the same behaviour for some cellular processes. In other processes, differences in their behaviour can be due to the different values of their components.

3.3. Interaction energy

The total interaction energy between similar particles as an addition of their electric, dispersive, and non-dispersive

Table 1
Surface tension and surface tension components (mJ/m^2) of liquids used in contact angle and thin layer wicking measurements (taken from Ref. [32]).

Liquid	γ	γ^{LW}	γ^+	γ^-
n-Decane	23.8	23.8	0	0
Formamide	58.0	39.0	2.28	39.6
Water	72.8	21.8	25.5	25.5

Table 2
Contact angles measurements with water, formamide, and diiodomethane; values of Lifshitz-van der Waals component (γ^{LW}); electron-acceptor γ^- and electron-donor γ^+ parameters of Acid/Base component of surface free energy for normal cells (mJ/m^2); total surface tension (γ^-).

	W / F / D	γ^{LW}	γ^+	γ^-	γ^{tot}
Fibroblasts	30°	28.6 ± 0.3	4.0 ± 0.1	42.6 ± 0.8	54.4 ± 0.8
Sol 8 p11	23°				
	60°				
Fibroblasts	21°	27 ± 2	3.0 ± 0.3	56 ± 1	52 ± 3
C2 C12 p10	30°				
	63°				

components was calculated. There is theoretical support for calculating the energy of interaction between particles and organs (heterocoagulation) when the surface properties of both are known [29,34].

Figs. 6 and 7 show the total interaction energy curves calculated from Table 1, Table 2, and Eqs. (4)–(6) and (9) in the Supplementary Materials, as a function of distance (H) from the surface, at a natural pH for normal cells. Changes in the aggregation dynamics might be characterised by the total potential interaction energy computed from the extended DLVO theory, including acid-base interactions (see Supplementary Materials).

Fig. 6 shows typical plots of the interaction energy ΔG_{131}^{TOT} between two identical cells (subscript 1) in a dispersion medium (subscript 3), and it shows the electrical, dispersive, and non-dispersive components as a function of their separation H (nm) from the cell surface. A negative ΔG_{131}^{TOT} indicates a primary or secondary energy minimum and an attractive force that produces colloid aggregation. In contrast, a positive sign implies a repulsive force that hinders it.

The electrostatic interaction (EL) will always give repulsive values between identical particles, which are strongly related to pH: the larger the zeta potential (absolute value), the stronger the repulsion. However, acid-base contribution can be attractive, repulsive, and even oscillatory in individual cases [35,36,37,38].

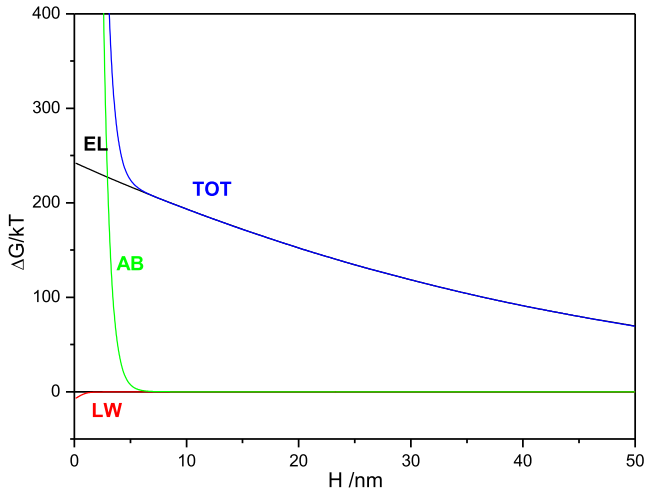

Fig. 6. Component of total interaction energy for normal cells (C2C12) at natural pH and 10^{-2} M of NaCl.

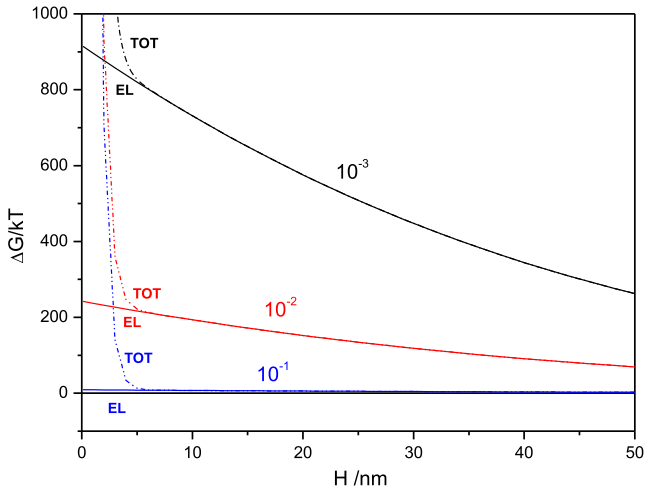

Fig. 7. Component of total energy interaction and electrical components for three ionic strength of Na^+ (10^{-1}, 10^{-2} and 10^{-3} M) at natural pH for line C2C12.

It accounts for a set of interactions that include, in addition to the typical non-dispersive ones, hydrogen bridges and hydrophilic attractions or hydrophobic structural repulsions. In the non-dispersive (AB) polar interaction, the monopolar and hydrophilic nature of the samples also causes net repulsion between particles according to Eqs. (8) and (9) in the Supplementary Materials. The AB repulsive force results from the excess in hydration pressure generated by the motion and orientation restrictions of water molecules on colloidal surfaces (hydration shells) because of hydrogen bonding [39]. In contrast, if the result for the AB interaction components were $\gamma^+ = 0$ and $\gamma^- < 28$ mJ/m^2, the character of the cells would have been hydrophobic. In this situation, "hydrophobic attraction" is produced; hence the values of AB interactions in Fig. 6 would be negative.

In this sense, the dispersive component (LW) always attracts (ΔG_{131}^{LW} negative). If the combined AB forces and the repulsive electrostatic forces are stronger than LW attraction, the overall interaction would be repulsive, and cell aggregates would tend to be mechanically unstable in a water medium. The stronger the repulsion, the greater the instability of aggregates [40].

From Figs. 6 and 7, it can be seen that the electrical component governs the coagulation processes between cells [41]; therefore, we now focussed only this component.

Fig. 7 shows the total interaction energy and its electrical component as a function of distance (H) for different ionic strengths of Na^+. For distances<5 nm, no large differences were observed in the obtained potential barriers. However, potential barriers were observed, indicating repulsion between cells that increases with a decrease in the distance between them, with a maximum at very short distances ($H \leq 5$ nm). These barriers increase with a decrease in ionic strength, likely due to an increase in zeta potential. A qualitative description suggests that for the natural pH (7.4), the potential barrier has values between 500 and 1500 kT. These values indicate repulsive behaviour between two nearby cells, and this repulsion may affect the generation of muscle mass and its functioning. Next, we studied the effect of other cations—Ca, Fe, and Al—using the same method. This method can also be used to study the effect of other common substances in the cellular medium.

The electrostatic interaction energy was compared for sodium and calcium for normal and tumour cells at a natural pH (Fig. 8). The calcium cation showed lower potential barriers than sodium. In general, the adsorption of calcium onto materials surface results in a lower zeta potential, as seen in Figs. 3 and 4. Moreover, the obtained values for the potential barrier for the Ca ion suggest the possibility of fibroblast aggregation. This behaviour is not possible for the Na ion as the barrier is over 250 kT. Finally, the results for tumour cells show very low potential energy barriers indicating greater aggregate stability.

A thorough analysis of the effect of the ionic strength (10^{-1}, 10^{-2}, 10^{-3} M) of sodium and calcium ions on the electrical energy of interaction for natural pH (7) has also been performed. The results have shown that for both cations a decrease in the ionic strength led to an increase in the potential barrier. This increase is higher in sodium than in calcium and is observed in both normal and tumor cells. However, there is a big difference, the maximum potential barrier does not reach 80 kT in tumour cells while in normal it can reach 900 kT (10^{-3} M of NaCl in both cases). On the contrary, with high ionic strengths (10^{-1} M) the barriers decrease, being smaller in tumour cells, what favours coagulation in tumour cells.

Therefore, we can even affirm that these variations in the potential barrier can be used to hinder the aggregation of these cells under some ionic concentrations.

Fig. 9 shows the potential curves obtained at different pH (4, 7, 9) with an ionic strength of 10^{-2} M. Fig. 9.a shows the results for normal cells, with potential barrier measurements for calcium substantially lower (<100 kT) than measures for sodium. In general, the repulsion increased with an increase in pH values, except for sodium, where the obtained barriers for pH = 4 were higher than those obtained for pH = 7.

In comparison, Fig. 9.b shows the results obtained for tumour cells. In this case, all potential barriers were lower than 100kT and were lower than for normal cells. Results for sodium stand out, where barriers of more than 250 kT decreased to less than 60 kT. The potential barriers obtained for calcium were much lower than measures for sodium, similar to normal cells, except for the sodium ion in a very acid pH.

Another notable observation for normal cells is that, in the case of calcium ions, an approximately 50% decrease in repulsion was observed with a pH decrease. While for tumour cells, the variation was also 50%; however, the effect was in the opposite direction. An increase in the potential barrier was observed with a decrease in pH.

For sodium ions, the high values obtained in potential barriers show the impossibility of aggregation for normal cells at all pHs. However, the barriers observed for tumour cells are much lower, indicating the possibility of aggregation, highlighting the almost disappearance of repulsion between these cells in acid medium (pH 4).

Obtaining zeta potential data for a trivalent cation at pH greater than 5 was not possible owing to the precipitate of a complex ion of aluminium and iron. In any case, the measurements and

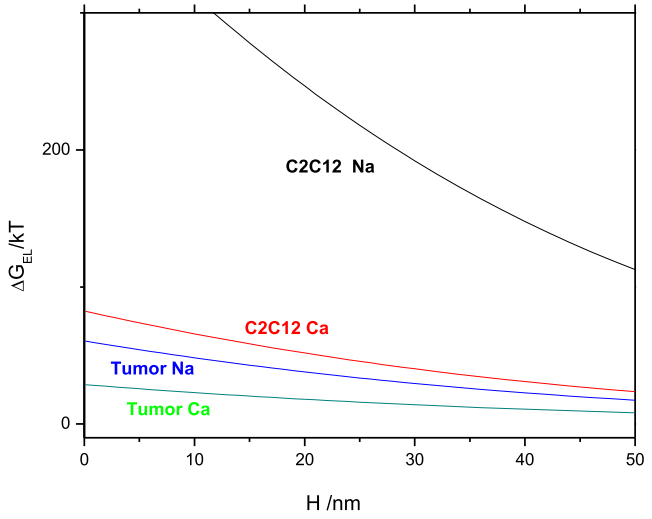

Fig. 8. Electrostatic component of interaction energy for normal and tumour cells at natural pH and 10^{-2} M of sodium and calcium ions.

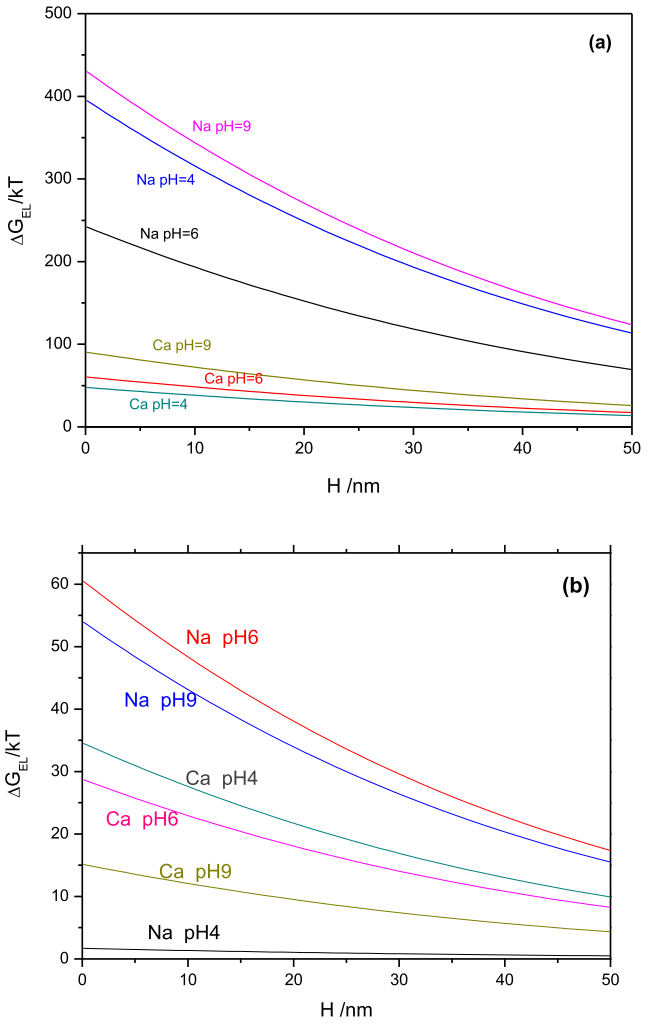

Fig. 9. Electrostatic component of interaction energy at different pH (4, 6, 9) with an ionic strength of 10^{-2} M of sodium and calcium ions: (a) cell line C2C12 and (b) breast tumour cells.

calculations have been made for pH = 4 with a concentration of 10^{-2} M of these ions. In general, the potential barriers increased with cation valence. Although, except for aluminium ions with normal cells, the obtained values for trivalent ions are higher than 200 kT, which leads us to think the particles will be very disaggregated. On the contrary, for mono and divalent ions the potential barriers are lower and very small for tumor cells. Hence, both sodium and calcium would allow aggregation, while the trivalent ions would result in the disaggregation of tumour cells.

4. Conclusions

The surface properties of normal and diseased cells are determinant in the phenomena of cell aggregation and the attachment of tumour cells to different tissues.

In general, the surface charge of cells is negative when the mono and divalent electrolytes are present in the ionic medium. In the case of trivalent ions and an acid pH the charge is reversed, probably related to precompensation of the charge near the charged surface. When the ionic concentration of electrolytes increases, the surface charge decreases. An increase in pH implies an increase in the surface charge.

The analysis of thermodynamics properties carried out with normal cell samples (C2C12 and Sol8P11) shows that they have a monopolar character, practically electron-donor in nature. This character confers a hydrophilic behaviour to cell surface.

In general, the higher ionic concentration of the medium implies a drastic decrease in the repulsion between the cells. When sodium and calcium ions are present, tumour cells remain aggregated at a given pH and concentration, while normal cells remain disaggregated.

The results show that the pH of the medium is a determining factor in the interaction energies between normal and diseased cells. This interaction is small enough in tumour cells to predict coagulation. In contrast, the potential barriers only allow coagulation in normal cells when the existing cation is calcium.

For normal cells, at a very acidic pH, where trivalent ions do not precipitate in complex ion forms, the aluminium ion was observed to provide coagulation, while the iron ion led to strong repulsion. In the case of tumour cells, the electrostatic repulsion between them increased with the cation valence.

Funding

This research received no external funding.

Declaration of Competing Interest

The authors declare that they have no known competing financial interests or personal relationships that could have appeared to influence the work reported in this paper.

Acknowledgments

we gratefully acknowledge the support of the institutions involved: the University of Jaén for the resources used; the "Liquid Biopsy and Cancer Interception" research group of the Genomics and Oncology Research Centre (GENYO) for providing the tumour cells used; UJA Research Group 'Cardiac and Skeletal Myogenesis: Muscle Regeneration (CTS 446) for providing the normal cells used.

Appendix A. Supplementary material

Supplementary data to this article can be found online at https://doi.org/10.1016/j.bioelechem.2021.108028.

References

[1] P. Sánchez-Moreno, J.L. Ortega-Vinuesa, A. Martín-Rodríguez, H. Boulaiz, J.A. Marchal-Corrales, J.M. Peula-García, Characterization of different functionalized lipidic nanocapsules as potential drug carriers, Int. J. Mol. Sci. 13 (2) (2012) 2405–2424.
[2] M.C. Leiva, R. Ortiz, G. Contreras-Cáceres, I. Perazzoli, J.M. Mayevych, F. López-Romero, J.M. Sarabia, C. Baeyens, J. Melguizo, Prados, Tripalmitin nanoparticle formulations significantly enhance paclitaxel antitumor activity against breast and lung cancer cells in vitro, Sci. Rep. 7 (2017), https://doi.org/10.1038/s41598-017-13816-z.
[3] A. Goldman, D. Bomze, R. Dankner, D. Fourey, B. Boursi, M. Arad, E. Maor, Cardiovascular Toxicities of Antiangiogenic Tyrosine Kinase Inhibitors: A Retrospective, Pharmacovigilance Study. Targeted Oncology. 16 (4) (2021) 471–483, https://doi.org/10.1007/s11523-021-00817-2.
[4] R.S. Ambekar, B. Kandasubramanian, A polydopamine-based platform for anticancer drug delivery, Biomaterials Sci. 7 (5) (2019) 1776–1793.
[5] S.S. Akhand, H. Chen, S.C. Purdy, Z. Liu, J.C. Anderson, C.D. Willey, M.K. Wendt, Fibroblast growth factor receptor facilitates recurrence of minimal residual disease following trastuzumab emtansine therapy, NPJ Breast Cancer 7 (1) (2021) 5.
[6] A. Jin, Y. Wang, K. Lin, L. Jiang, Nanoparticles modified by polydopamine: Working as "drug" carriers, Bioactive Mater. 5 (3) (2020) 522–541, https://doi.org/10.1016/j.bioactmat.2020.04.003.
[7] I. Dobrzyńska, B. Szachowicz-Petelska, Z. Figaszewski, S. Sulkowski, Changes in electric charge and phospholipid composition in human colorectal cancer cells, Mol. Cell. Biochem. 276 (2005) 113–119.
[8] I. Dobrzynska, E. Skrzydlewska, Z. Figaszewski, Parameters characterizing acid–base equilibria between cell membrane and solution and their application to monitoring the effect of various factors on the membrane, Bioelectrochemistry 69 (2) (2006) 142–147.
[9] I. Dobrzyńska, J. Kotyńska, Z. Figaszewski, Changes in electrical charge of phosphatidylcholine and phosphatidylserine liposomal membranes caused by adsorption of monovalent ions, Chem. Anal 52 (2007) 931–944.
[10] I. Dobrzynska, E. Skrydlewska, Z.A. Figaszewski, Changes in electric properties of human breast cancer cells, J. Membrane Biol. 246 (2013) 161–166, https://doi.org/10.1007/s00232-012-9516-5.
[11] Ram Dhan Yadav, Abha Chaudhary. Nano-bio surface interactions, cellular internalisation in cancer cells and e-data portals of nanomaterials: A review. IET Nanobiotechnology.
[12] C. Bingdi, L. Wenjun, W. Yilong, et al., Targeting negative surface charges of cancer cells by multifunctional nanoprobes, Theranostics 6 (I) (2016), https://doi.org/10.7150/thno.16358.
[13] P. Daubas, A. Klarsfeld, I. Garner, C. Pinset, R. Cox, M. Buckingham, Functional-activity of the 2 promoters of the myosin alkali light chain gene in primary muscle-cell cultures - comparison with other muscle gene promoters and other culture systems, Nucleic Acids Res. 16 (4) (1988) 1251–1271, https://doi.org/10.1093/nar/16.4.1251.
[14] David Yaffe, Ora Saxel, Serial passaging and differentiation of myogenic cells isolated from dystrophic mouse muscle, Nature 270 (5639) (1977) 725–727.
[15] H.M. Blau, G.K. Pavlath, E.C. Hardeman, C.-P. Chiu, L. Silberstein, S.G. Webster, S.C. Miller, C. Webster, Plasticity of the differentiated state, Science 230 (4727) (1985) 758–766.
[16] S. Martínez-Fernandez, F. Hernández-Torres, D. Franco, G.E. Lyons, F. Navarro, A.E. Aránega, Pitx2c overexpression promotes cell proliferation and arrests differentiation in myoblasts, Dev. Dyn. 235 (11) (2006) 2930–2939.
[17] E. Lozano-Velasco, D. Vallejo, F.J. Esteban, C. Doherty, F. Hernández-Torres, D. Franco, A.E. Aránega, Pitx2 modulates cell proliferation in myoblasts and skeletal-muscle satellite cells and promotes their commitment to a myogenic cell fate, Mol. Cell. Biol. 35 (2015) 2892–2909.
[18] S. McLaughlin, The electrostatic properties of membranes Ann, Rev. Biophys. Biophys. Chem. 18 (1989) 113–136.
[19] I. Bernhardt et al., Influence of surface charge and transmembrane potential on rubidium-86 efflux of human red blood cells, J. Membr. Biol. 78 (3) (1984) 249–255.
[20] A. Iglic, M. Brumen, S. Svetina, Determination of inner surface potential of the erythrocyte membrane, Bioelectrochem. Bioenerg. 43 (1997) 97–103.
[21] D.F. Evans, H. Wennerstrom, The Colloidal Domain: Where Physics, Chemistry, Biology, and Technology Meet, Wiley-VCH, New York, 1999.
[22] K. Dołowy, Bioelectrochemistry of cell surface, Progress in Surface Sci. 15 (1984) 245–368.
[23] B. Szachowicz-Petelska, I. Dobrzynska, M. Skrodzka, B. Darewicz, Z.A. Figaszewski, J. Kudelski, Phospholipid Composition and Electric Charge in Healthy and Cancerous Parts of Human Kidneys, J. Membrane Biol. 246 (5) (2013) 421–425.
[24] G. Gogichadze, T. Gogichadze, E. Misabishvili, et al., Possible effect of variable membrane potential of a cancer cell on different carcinogenic processes, Georgian Med. News. 234 (2014) 116–120.

[25] K.M. Lipman, R. Dodelson, R.M. Hays, The surface charge of isolated toad bladder epithelial cells mobility, effect of pH and divalent ions, J. General Physiol. 49 (1966) 501–516.
[26] N. Cuvillier, F. Rondelez, Breakdown of the Poisson-Boltzmann description for electrical double layers involving large multivalent ions, Thin Solid Films. 327–329 (1998) 19–23.
[27] V. Aranda, J. Calero, I. Plaza, A. Ontiveros-Ortega, Long-term effects of olive mil pomace co-compost on wettability and soil quality in olive groves, Geoderma 267 (2016) 185–195.
[28] A. Ontiveros-Ortega, F. Vidal, E. Giménez, J.M. Ibañez, Effect of heavy metals on the surface free energy and zeta potential of volcanic glass: implication on the adhesion and growth of microorganism, J. Mater. Sci. 49 (2014) 3550–3559.
[29] A. Ontiveros, J. Duran, A.V. Delgado, F. Gonzalez-Caballero, E. Chibowski, A study on the adhesion of calcium carbonate to glass. Energy balance in the deposition process, J. Adhesion Sci. & Technol. 10 (1996) 847–868.
[30] J.A. Moleón, A. Ontiveros-Ortega, E. Gimenez, I. Plaza, Effect of NCPCL in the adsorption process of graphene oxide onto polyester, Dyes and Pigments. 122 (2015) 310–316.
[31] C.J. Van Oss, R.J. Good, Surface tension and the solubility of polymers and biopo-lymers: the role of polar and apolar interracial free energy, J. Macromol. Sci.: Pure Appl. Chem. 26 (1989) 1183–1203.
[32] C.J. Van Oss, M.K. Chaudhury, R.J. Good, Interfacial Lifshitz-van der Waals and Polar Interactions in Macroscopic Systems, Chem. Rev. 88 (1988) 927.
[33] C.J. Van Oss, Interfacial Forces in Aqueous Media, Dekker, New York, 1994.
[34] J.D.G. Duran, A. Ontiveros, E. Chibowski, Kinetics and interfacial interactions in the adhesion of colloidal calcium carbonate to glass in a packed-bed, Appl. Surf. Sci. 134 (1998) 125–138.
[35] J. Urbanija, K. Bohinc, A. Bellen, S. Maset, A. Iglič, V. Kralj-Iglič, Sunil Kumar, Attraction between negatively charged surfaces mediated by spherical counterions with quadrupolar charge distribution, J. Chem. Phys. 129 (2008).
[36] S. Perutkova, M. Frank, K. Bohinc, G. Bobojevic, J. Zelko, B. Rozman, V. Kralj-Iglic, A. Iglic, Interaction Between Equally Charged Membrane Surfaces Mediated by Positively and Negatively Charged Macro-Ions, J. Membrane Biol. 236 (2010) 43–53.
[37] J. Israelachvili, Intermolecular and surface forces, Academic, London, 1991.
[38] E.R. Levin, Cellular functions of plasma membrane estrogen receptors, Steroids 67 (6) (2002) 471–475, https://doi.org/10.1016/s0039-128x(01)00179-9.
[39] J. Zelko, A. Iglič, V. Kralj-Iglič, P.B.S. Kumar, Effects of counterion size on the attraction between similarly charged surfaces, J. Chem. Phys. 133 (20) (2010) 204901, https://doi.org/10.1063/1.3506896.
[40] R.C. Plaza, L. Zurita, J. Duran, F. Gonzalez-Caballero, A.V. Delgado, Surface termodynamics of Hematite/Yttrium Oxide Core-Shell colloidal particles, Langmuir 14 (1998) 6850–6854.
[41] T. Osaka, T. Nakanishi, S. Shanmugam, S. Takahama, H. Zhang, Effect of surface charge of magnetite nanoparticles on their internalization into breast cancer and umbilical vein endothelial cells, Colloids Surf., B 71 (2) (2009) 325–330.